Geophysical Research Letters

RESEARCH LETTER
10.1029/2020GL087907

Jet Speed Variability Obscures Euro-Atlantic Regime Structure

J. Dorrington[1] and K. J. Strommen[1]

[1]Department of Physics, University of Oxford, Oxford, UK

Key Points:
- The approximately Gaussian jet speed serves to obscure non-Gaussian regime structure in the phase space of geopotential height
- If this influence is removed, the regime structure becomes significantly more robust and stable across the entire twentieth century
- We find a new paradigm of three main regimes that can be consistently extended to five regimes, capturing both jet latitude and blocking patterns

Supporting Information:
- Supporting Information S1

Correspondence to:
K. J. Strommen,
kristian.strommen@physics.ox.ac.uk

Citation:
Dorrington, J., & Strommen, K. J. (2020). Jet speed variability obscures Euro-Atlantic regime structure. *Geophysical Research Letters*, *47*, e2020GL087907. https://doi.org/10.1029/2020GL087907

Received 10 MAR 2020
Accepted 15 JUN 2020
Accepted article online 15 JUN 2020

Abstract Euro-Atlantic regimes are typically identified using either the latitude of the North Atlantic jet or clustering algorithms in the phase space of 500-hPa geopotential (Z500). However, while robust trimodality is visibly apparent in jet latitude indices, Z500 clusters require highly sensitive significance tests to distinguish them from autocorrelated noise. This leads to considerable decadal variability in regime patterns, confounding many potential applications. A clear-cut choice of the optimal number of regimes is also hard to justify. We argue that the jet speed, a near-Gaussian distribution projecting strongly onto the Z500 field, is the source of these difficulties. Once its influence is removed, the phase space becomes visibly non-Gaussian, and clustering algorithms easily recover three regimes, closely corresponding to the jet latitude modes. Further analysis supports the existence of two additional blocking regimes, corresponding to a tilted and split jet. All five regimes are approximately stationary across the twentieth century.

Plain Language Summary Weather over the North Atlantic region during winter is highly variable, with shifts in the jet stream and anticyclonic blocks both having large impacts on western Europe. A common way of thinking about this variability is in terms of movement between persistent large-scale weather patterns termed *regimes*. However, settling on an optimal and consistent set of regime patterns has proved very challenging. We show that by removing the influence of jet speed from the geopotential height field, it is much easier to identify stable regime patterns, which well describe observations. These patterns include both jet dynamics and blocked states, forming a bridge between previous studies that looked for regimes in either the jet latitude or geopotential height in isolation.

1. Introduction

One way to understand variability in the Euro-Atlantic circulation is through the study of non-Gaussian structure in its phase space, which indicates preferred flow configurations. Many studies have found evidence to suggest the existence of such deviations from Gaussianity, manifesting themselves in the form of quasi-persistent weather regimes (e.g., Michelangeli et al., 1995; Vautard, 1990, and discussion within for early history; more recently see, e.g., Cassou, 2008; Franzke et al., 2011; Hannachi et al., 2017; Straus, 2010; Straus et al., 2007; Woollings, Hannachi, Hoskins, & Turner, 2010; Woollings, Hannachi, & Hoskins, 2010). Their importance in modulating European weather is now well documented (Ferranti et al., 2015; Frame et al., 2013; Matsueda & Palmer, 2018), and, conjecturally, they may critically influence the regional response to anthropogenic forcing (Corti et al., 1999; Palmer, 1999). From the perspective of weather forecasting, they offer a tantalizingly simple truncation of the atmosphere to Markovian dynamics (Ghil & Robertson, 2002; Strommen & Palmer, 2019).

There are two main approaches in the literature for diagnosing Euro-Atlantic regimes. The most commonly used method is to apply clustering algorithms to geopotential height data at 500 hPa (Z500). This typically produces four regimes: the positive and negative North Atlantic Oscillation (NAO), an Atlantic ridge, and a Scandinavian blocking pattern (Cassou, 2008; Dawson et al., 2012; Strommen et al., 2019). However, two problems emerge in this framework. Firstly, the choice of exactly four regimes depends on complicated statistical significance testing, which is typically highly sensitive to the inclusion or removal of small numbers of points. While this is a particularly serious complication when evaluating regimes on centennial time scales, a shift in the time period considered by as little as 4 years can mean the difference between statistical significance or not, even when restricting to the satellite era (Strommen et al., 2019). For models, which appear to struggle to replicate good regime structure, this sensitivity is considerably magnified. Secondly, as we will show in this paper, the four regimes are highly unstable across the twentieth century,

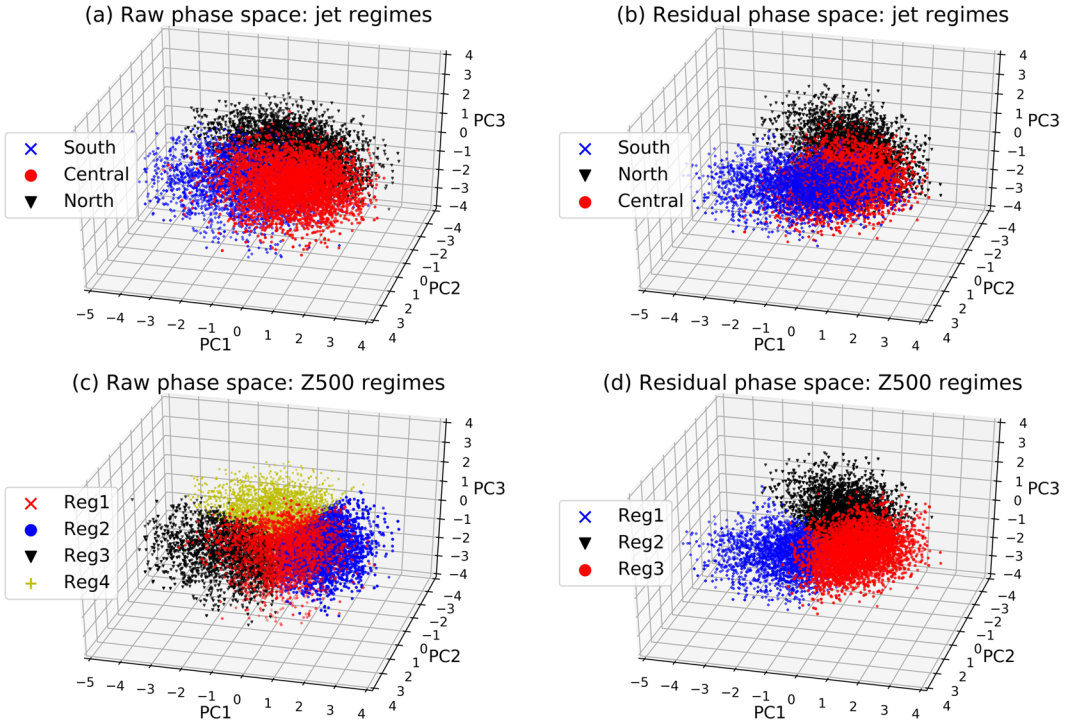

Figure 1. Projections of the Z500 phase space of ERA20C onto the first three EOFs. In (a) and (c) is shown the raw phase space with points marked according to the jet latitude regimes in (a) and according to the K-means cluster regimes in (c). In (b) and (d) is shown the residual phase space (i.e., with the jet speed removed), with points in (b) marked by jet latitude regimes and (d) by clustered regimes. In (c), the regimes shown are NAO+ (Reg1), NAO− (Reg2), Atlantic Ridge (Reg3), and Scandinavian Blocking (Reg4).

exhibiting significant decadal fluctuations in their spatial patterns. While this may ostensibly be a feature of the climate system, it calls into question the use of these regimes for many applications.

Arguably, the underlying issue responsible for all this ambiguity is the fact that the Z500 phase space is not visually distinguishable from Gaussian noise (see, e.g., Figure 1a of this paper). This is in stark contrast to the other common way of identifying Euro-Atlantic regimes by appealing to the eddy-driven jet. Indeed, in Woollings, Charlton-Perez, et al. (2010), a simple computation of the daily latitude of the jet produces a visibly trimodal histogram, suggesting the existence of three distinct jet regimes without the need for further significance testing. Furthermore, these jet regimes are notably stable, showing little sensitivity to the choice of time period used or subsetting of data. The work in Madonna et al. (2017) went a long way toward reconciling these with the Z500 regimes discussed above, by identifying the three jet regimes with three of the four Z500 regimes. It was showed that the "missing" fourth regime (Scandinavian blocking) corresponds to either a tilted or split jet, not captured by the strictly zonal jet latitude index. However, these could only be cleanly separated by extending to five regimes, seemingly at odds with studies supporting only four robust regimes. If these two perspectives are capturing the same underlying structure, why are stable and robust centennial Z500 regimes so much harder to diagnose than the corresponding jet regimes, and why is translation between the two not more straightforward?

In this paper we argue that the confounding factor obscuring Euro-Atlantic regime structure is the jet speed. It is well known that the NAO, the leading principal component (PC) of Z500 during December-January-February (DJF), enjoys strong linear correlation with the jet speed, which is to good approximation, Gaussian in its distribution (Parker et al., 2019). In fact, this is the case for the other PCs as well, and once the influence of the jet speed has been regressed out, we show that one is left with a visibly non-Gaussian phase space. By applying K-means clustering algorithms to this new phase space, we find clear support for either three or five regimes. The choice K=3 corresponds naturally to the three jet latitude regimes, while K=5 adds regimes corresponding to a split and tilted jet, thereby justifying the bridge between the jet and

Z500 regimes proposed in Madonna et al. (2017). In both cases, the regime patterns are considerably more stable across the entire twentieth century than when clustering unregressed PCs.

We argue that separating out the influence of the jet speed in this manner is therefore a natural and beneficial step when analyzing Euro-Atlantic circulation, and adds considerable clarity to how the two regime pictures are related.

In section 2 we present the data used and describe the relevant computational methodologies. In section 3 we present the results and in section 4 draw our conclusions.

2. Data and Methods

2.1. Data

Because we will be interested in understanding the stability of regimes on decadal time scales, the long reanalysis data set ERA20C (Poli et al., 2013) is used, which covers the period 1900–2010. ERA20C assimilates only surface observations, but because both Z500 and the jet are tightly constrained by surface pressure alone, its representation of both is not appreciably different from reanalysis data assimilating satellite data. Indeed, using the full time period reproduces the same regime behavior, both in terms of the jet and Z500, more commonly identified using modern reanalysis data sets covering the period 1979 onward. This data set, also used in Parker et al. (2019), was therefore deemed suitable for our purposes.

We will be working with daily Z500 fields and 850-hPa zonal wind fields (U850) covering DJF 1901/1902 to 2010/2011 and will compute regimes both for the full period, as well as for different 30-year windows.

2.2. Methods

A low-dimensional truncation of the full Z500 phase space is obtained as in Dawson et al. (2012). Concretely, we calculate the leading 10 PCs of area-weighted Z500 restricted to the Euro-Atlantic sector [80°W to 40°E, 30–90°N] and DJF, over the full date range 1901–2010, with a seasonal cycle removed from each grid point. The computed PCs explain 83.5% of the total variance. To make plots more readable, the PCs were standardized by dividing all of them by 10^4.

Jet latitude and jet speed time series are computed using the simplified methodology described in Parker et al. (2019). Daily zonal means of zonal winds are restricted to the region [0–60°W, 15–75°N] and 850 hPa, before being smoothed with a 9-day running mean. For each day of the DJF season, the speed of the jet is defined as the maximum wind speed attained in this domain and the latitude of the jet is the latitude at which this maximum is located. As noted in ibid, this procedure produces qualitatively similar results to more complex methods using winds at multiple levels and/or additional filtering.

Clustering is always done with a standard K-means algorithm, which produces clusters that maximize the *optimal ratio*:

$$\frac{\textit{Intercluster variance}}{\textit{Intracluster variance}}, \tag{1}$$

where the intercluster variance refers to the variance between the cluster centroids (weighted by the number of points in each cluster) and the intracluster variance refers to the average variance of the differences between the cluster centroids and the datapoints associated to that cluster. A large intercluster variance therefore implies that the centroids are well separated from each other, while a small intracluster variance implies the points of each cluster are located close to their respective centroid. Consequently, a large optimal ratio is associated with a more clearly robust regime structure.

One of the long-standing issues with applying clustering to atmospheric data is the inability to choose a cluster number a priori. A commonly used method for identifying cluster number a posteriori is the Bayesian information criterion (BIC), which we will employ in this paper. This aims to minimize the residual unexplained variance of the data set while attempting to account for overfitting by penalizing large numbers of free parameters (Fraley et al., 1998). In the context of K-means clustering, this takes the form:

$$BIC = \sum_{n}^{N} \underset{K}{\operatorname{argmin}} \left(\|X_K - x_n\|^2 \right) + KD \cdot \log(N). \quad (2)$$

The first term is the sum of squared distances of each of the N datapoints to the nearest of the K clusters, with centroids X_K (the intracluster variance above). The second term is our parameter penalization, where D is the state-space dimension and where the logarithmic scaling with N follows from information theoretic arguments (Schwarz, 1978).

3. Results

We show how removing the imprint of the jet speed alters the structure of the Z500 phase space and diagnose regimes in this residual space.

3.1. Removing the Signature of the Jet Speed

The daily jet speed index enjoys statistically significant correlation with the first two PCs of Z500, at approximately 0.44 and 0.49, respectively. Correlations with further PCs decrease rapidly, implying that most of the jet speed variability is captured by the NAO (first PC) and the East Atlantic pattern (second PC), in line with the results of Woollings, Hannachi, and Hoskins (2010): See Figure S1 in the supporting information (SI).

Because the influence of the jet speed on the PCs is linear to good approximation, we remove it from the Z500 phase space using linear regression. Concretely, the jet speed is regressed against each of the 10 PCs separately; the residuals of this regression form the coordinate vectors of a new phase space where the jet speed, by construction, does not correlate with any of them. We call this the *residual phase space*. Because the jet speed correlates strongly with the NAO, the linear field being removed in this manner resembles a positive NAO (see Figure S2 in the SI).

The impact of this procedure can be seen in Figure 1 (see also Figure S3 in the SI for a version with no coloring). In (a) and (c) are shown a projection of the 10-dimensional phase space onto the first three empirical orthogonal functions (EOFs). In (a), the points have been colored according to which of the three jet latitude regimes they belong to, while in (c), the coloring is done according to the "classical" regimes identified by K-means clustering with $K = 4$. The phase space does not exhibit deviations from Gaussianity easily visible to the human eye. By contrast, (b) and (d) show the residual phase space, where non-Gaussian structure is clearly identifiable. Once again, in (b) the color indicates the three jet regimes, while in (d), the color indicates the regimes identified by K-means clustering of the residual phase space with $K = 3$. It can be seen that the K-means clustering essentially reproduces the three jet regimes, a correspondence we will quantify in section 3.2. In fact, the curvature visible in Figures 1b and 1d corresponds exactly to the nonlinear relationship between the jet latitude and the NAO first observed in Woollings, Hannachi, and Hoskins (2010): See also Figure 2 of Strommen (2020), where this nonlinearity is more clearly highlighted.

This lends compelling evidence toward the idea that the regimes in the Z500 phase space are simply an imprint of the three jet latitude regimes. However, it is still possible that $K = 3$ is not the optimal choice of clusters for the residual phase space. We address this next.

3.2. Identifying the Optimal Regime Structure

We now consider the question of identifying the optimal number of regimes in this residual phase space. Due to the visible non-Gaussian structure, conventional significance testing based on the cluster sharpness (Dawson et al., 2012; Strommen et al., 2019) always produces regimes that are 100% significant against a null hypothesis of autocorrelated noise, in stark contrast to the raw phase space.

A consequence of this is, however, that we can no longer use this test to assess the number of regimes. Instead, we consider two alternative metrics. The BIC is an information theoretic measure of model suitability, as discussed in section 2, and the minima of the BIC can be used to identify the optimal number of free parameters in a model, which in our case is precisely the cluster number. Figure 2a shows that a broad minima exists for both raw and residual PCs when using $K = 5$ or 6, which is consistent with the findings of, for example, Falkena et al. (2019). Both data sets have had their variance normalized prior to

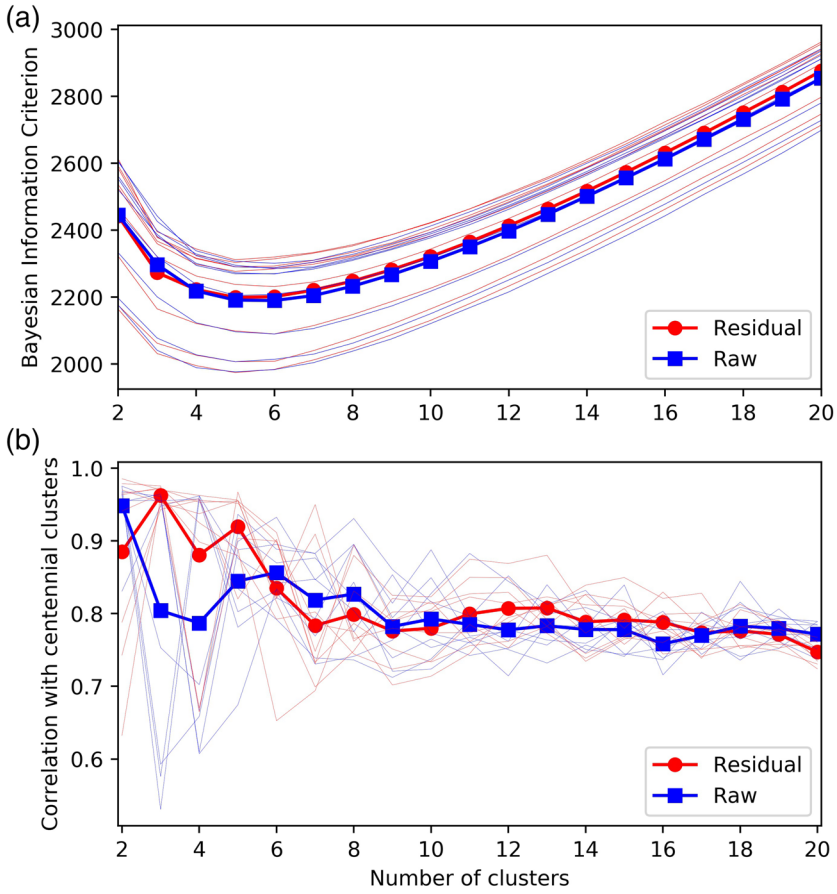

Figure 2. (a) The BIC for varying numbers of K-means clusters found in the residual phase space (red) and the raw phase space (blue). Thin lines show results for each of the 30-year windowed periods, with the mean indicated by the thick lines. (b) Thin lines show the average full-field pattern correlation of cluster composites between each 30-year window of data and the full centennial data set. Again, the thick lines indicates the mean of the windowed results.

clustering and we see that the absolute value of the BIC, and its structure as a function of cluster number is essentially unchanged by our regression procedure; the statistical validity of a multimodal hypothesis appears unchanged.

However, the BIC is only one of many proposed methodologies for selecting regime number, which can often give conflicting results, and we must bear in mind its underlying formal assumptions that our data violate, particularly the conditions of stationarity and independence. We are therefore prompted to consider a more physically grounded, domain-specific metric that reflects the intended reason for identifying regimes in the first place. In our case, it is highly desirable for dynamically relevant regimes to be approximately stationary features of the midlatitude circulation over centennial time scales, at least in terms of spatial patterns if not in residence times or transition probabilities. This desire is also rooted in expectations from lower-dimensional systems, such as Lorenz '63, where changes to the forcing do not result in changes to the spatial patterns of the regimes (the wings of the butterfly) but rather to changes in the residence time (Palmer, 1999).

To that end, we define a stationarity metric by calculating the average area-weighted pattern correlation between clusters found in rolling 30-year windows of our data set and those found in the full centennial data set. We use nine windows, [1902–1931, 1912–1941, ...1982–2010], and in each case find the bijection between windowed and centennial clusters that maximizes the pattern correlation of the regime composites. The results of this are shown in Figure 2b, for both raw and residual PCs.

Using raw PCs we see strong stationarity for $K = 2$, representing the NAO dipole (not shown), followed by a considerable drop in stationarity for larger cluster numbers, with a local maximum correlation of 0.85 for

$K = 6$. As cluster number increases further the correlation asymptotes to a value of 0.78. For the commonly used choice $K = 4$ the stationarity is close to this low asymptotic value but shows considerably more variability in correlation dependent on time window, suggesting that this is a result of shifts in the four dominant regime structures over the century.

When using residual PCs, we see the same asymptotic behavior for large clusters as in the raw PC case, and reduced stationarity for $K = 2$, which is to be expected as we have deliberately removed an NAO+ like pattern from our data. However, we see high stationarity emerge for $K = 3$ and 5, with correlations exceeding 0.9, followed by a sharp decline in stationarity for six or more clusters. This high stationarity is particularly notable for $K = 3$, with no window showing a correlation lower than 0.96. This is a desirable outcome not only because it means we can find exceptionally stable clusters that can be used in different time periods but also because it suggests a clear way to rule out large cluster numbers, something which has proven difficult in earlier regime studies. This increased stability is in accordance with the observation in Woollings et al. (2014) that while jet speed shows statistically significant interdecadal variability, the jet latitude does not. Removing the influence of the jet speed would therefore be expected to reduce decadal variability.

3.3. The Case $K = 3$: Jet-Analog Regimes

In Figure 3 we look at the Case $K = 3$. While it does not represent minima of the BIC, the regime clusters are highly stable across the twentieth century and appear to correspond closely to the three jet latitude regimes. We therefore examine these clusters in more detail.

From the geopotential anomaly composites associated with each cluster, seen in Figure 3a, we label these as a blocking/NAO+ hybrid (BLK/NAO+), a pure NAO− pattern, which can also be thought of as Greenland blockings, and an Atlantic ridge/NAO+ hybrid (AR/NAO+) by analogy to the four traditional Euro-Atlantic regime. This identification holds quantitatively, as we can see if we look at the coincidence matrix which encodes how many days assigned to a regime i under one clustering framework are assigned to a regime j under a different set of regime classifications:

$$\begin{array}{c} \\ BLK/NAO+ \\ NAO- \\ AR/NAO+ \end{array} \begin{array}{c} \begin{array}{cccc} BLK & NAO+ & NAO- & AR \end{array} \\ \begin{bmatrix} 2,103 & 1,785 & 65 & 229 \\ 264 & 128 & 1,772 & 125 \\ 102 & 1,045 & 200 & 1,992 \end{bmatrix} \end{array}.$$

The corresponding zonal wind composites, displayed in Figure 3b, show that the projection onto the jet is considerable. Our NAO− cluster is linked to a southerly jet, the AR/NAO+ with a northerly jet, while the AR/BLK pattern is characterized mainly by a weak jet over western Europe that tilts from southwest to northeast. Full fields are shown in Figure S8.

The similarity matrix below shows how similar the assignment of days is for the jet latitude clusters and the clusters in residual Z500 obtained here. We see that approximately 60% of the days assigned to each Z500 regime come from a single jet regime, as expected from the visual similarity apparent in Figure 1:

$$\begin{array}{c} \\ BLK/NAO+ \\ NAO- \\ AR/NAO+ \end{array} \begin{array}{c} \begin{array}{ccc} Central & Southern & Northern \end{array} \\ \begin{bmatrix} 2,290 & 606 & 1,286 \\ 672 & 1,483 & 134 \\ 1,209 & 141 & 1,989 \end{bmatrix} \end{array}$$

The statistics of regime lifetime, displayed in Figure 3c, show a strongly Markovian persistence structure, with a typical lifetime of around 1 week and with rare monthlong regime events occurring for all clusters at some point in the centennial record. Given the strong Markovianity, there is value in examining the transition matrix, which defines the daily probability of moving from one cluster to another:

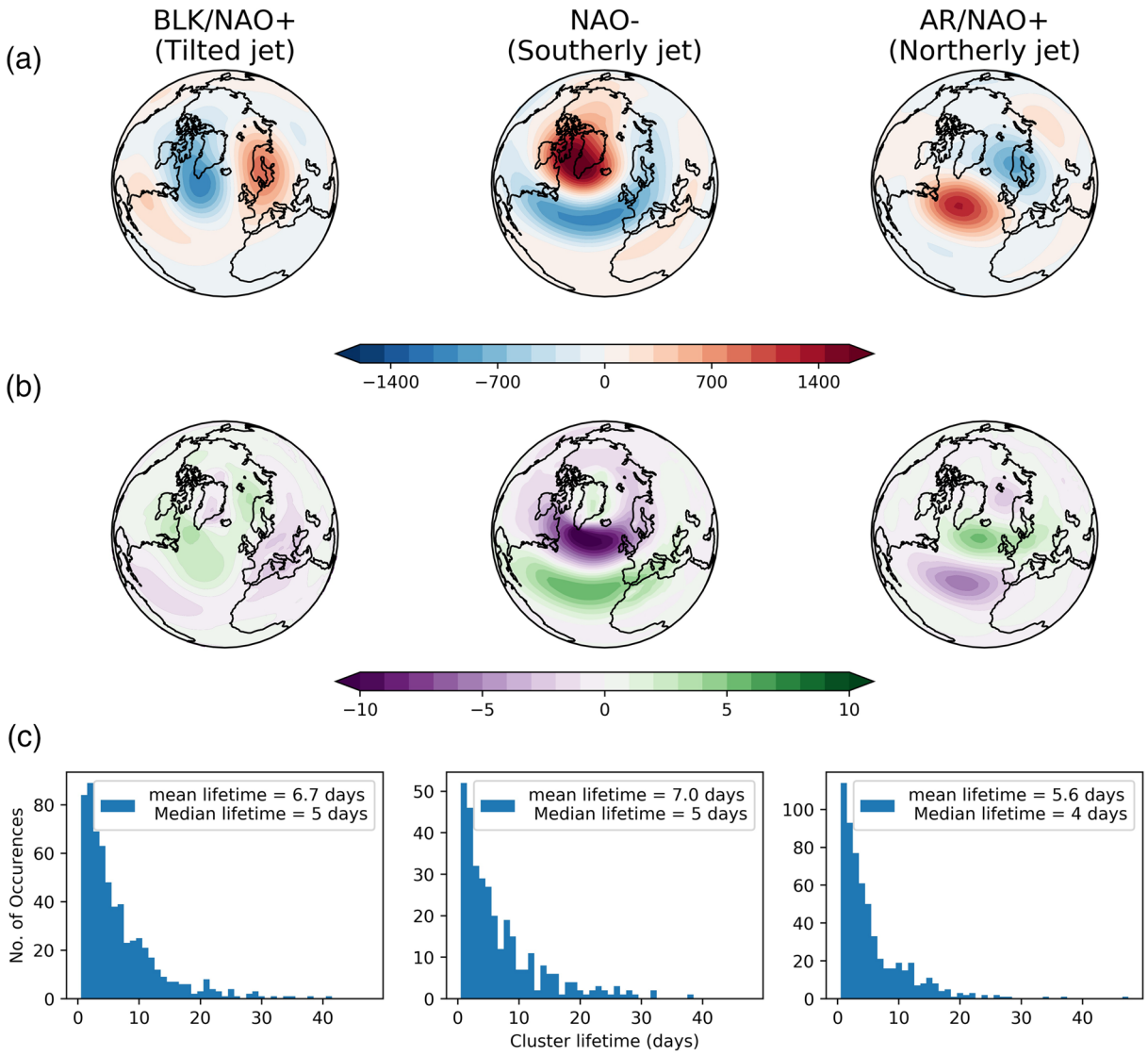

Figure 3. Clusters composites for K-means clusters found using K=3 in residual PCs of DJF Z500 1902–2010. Composites of Z500 anomalies for days assigned to each regime are shown in (a), while composites of U850 anomalies are shown in (b). Histograms of cluster lifetime are shown in (c).

$$
\begin{array}{lc}
\textit{From} \downarrow \textit{To} \rightarrow & \begin{array}{ccc} BLK/NAO+ & NAO- & AR/NAO+ \end{array} \\
\begin{array}{l} BLK/NAO+ \\ NAO- \\ AR/NAO+ \end{array} & \left(\begin{array}{ccc} 0.85 & 0.04 & 0.11 \\ 0.08 & 0.86 & 0.06 \\ 0.13 & 0.05 & 0.82 \end{array} \right)
\end{array}
$$

This is strongly inhomogeneous (a desirable trait if regimes are to be used for predictive purposes), with transitions into the NAO− state much less common than transitions between the two hybridized NAO+ states. This bears similarities to the transition matrix found for clusters of the jet latitude index such as in (Franzke et al., 2011), where the northern and central jet states prefer to transition to each other.

3.4. The Case K=5: Extended Jet Regimes

While the variability of the jet latitude seems to be well described by a trimodal structure, if we also want to capture the range of Atlantic blocking dynamics we may benefit from extending our basis of regimes. In

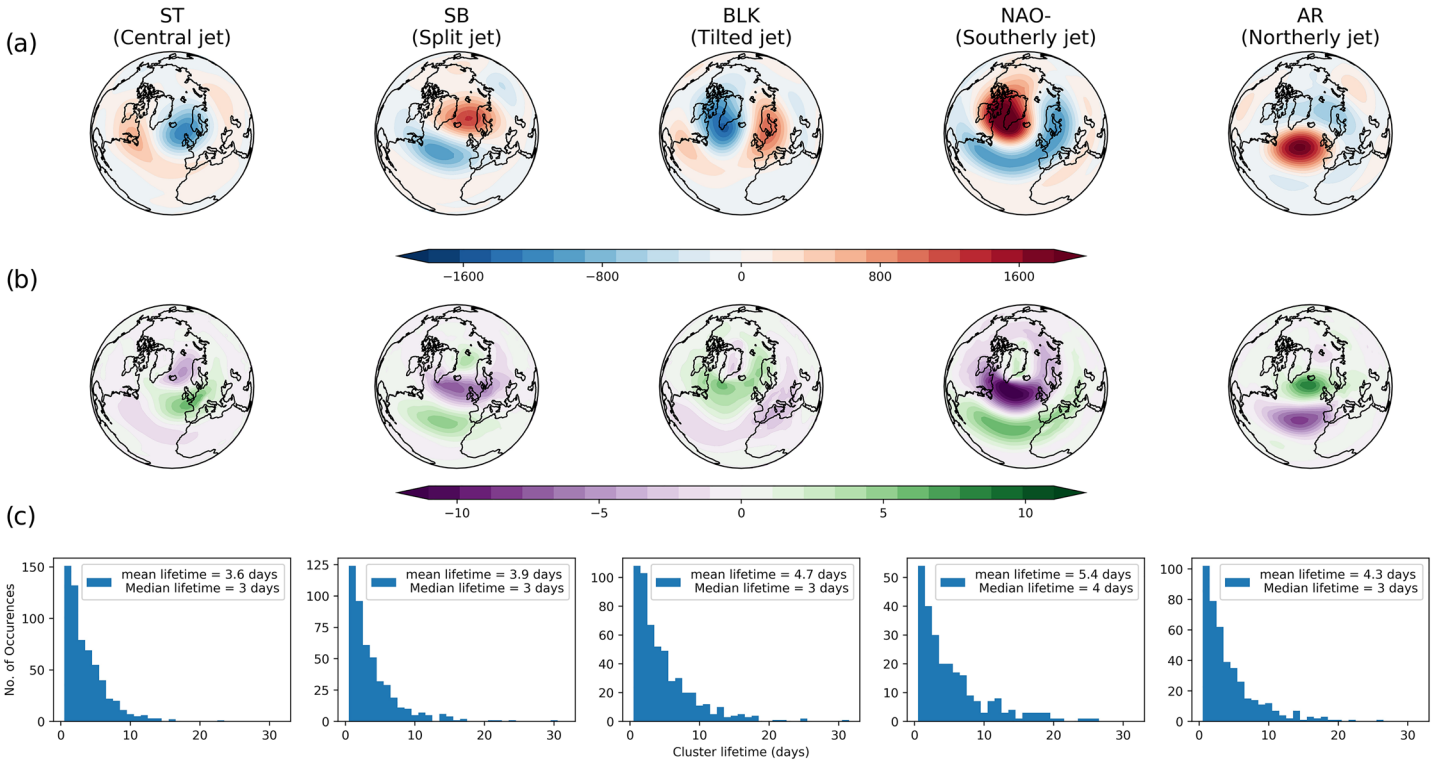

Figure 4. As for Figure 3 but using K=5.

particular, Scandinavian blocking shows trademarks of quasi-persistent dynamics and persistent blocking in general provided the motivation behind early work on weather regimes (Vautard, 1990).

A choice of five regimes also showed strong stationarity in Figure 2 while also representing a minima of the BIC. This justifies an extension to five regimes, with the resulting composites in Figure 4 (full field composites are shown in Figure S9).

The two new regimes, Clusters 1 and 2 here, are hybrids: Cluster 1 is 64% AR, 26% BLK/NAO+, and 10% NAO−, while Cluster 2 is 57% NAO+/BLK and 39% NAO−. We call these a Scandinavian trough and Scandinavian block respectively (abbreviated to ST and SB) in allusion to the similar patterns found in Beerli and Grams (2019). This information can be read off from the similarity matrix:

$$\begin{array}{c} \\ BLK/NAO+ \\ NAO- \\ AR/NAO+ \end{array} \begin{array}{c} \begin{array}{ccccc} ST & SB & BLK & NAO- & AR \end{array} \\ \begin{bmatrix} 570 & 1,038 & 3,509 & 0 & 65 \\ 223 & 709 & 0 & 1,339 & 18 \\ 1,397 & 81 & 42 & 49 & 1,770 \end{bmatrix} \end{array}$$

Clusters 1, 4, and 5 map onto the central, southern, and northern jet latitude regimes, while Clusters 2 and 3 represent flows with a split and tilted jet, respectively. This can be seen in more detail in Figures S5 and S6, which show explicitly the distribution of jet latitudes in each regime, and show the more localized blocking character of the SB and BLK regimes which are partially decoupled from jet position.

These five regimes are a straightforward extension of the three regimes in the previous section, adding extra detail but not removing any prior patterns. In particular, we recover all five jet regimes discussed in Madonna et al. (2017), thereby justifying the separation of the mixed regime they find there into split and tilted jet states. The full transition matrix is shown in Table S1. The ability to capture both the full set of jet regimes and blocking patterns in a stable and reproducible way across the entire century is a noteworthy feature that derives from our residual clustering approach and sets it apart from previous studies on regime identification. A visualization of how the five clusters are positioned in phase space is provided in Figure S4 of the SI.

We might ask why, despite their popular use in previous work, four regimes do not seem as appropriate here. When setting K=4 in our residual space, we found K-means clustering consistently returns Clusters 3, 4, and 5 of Figure 4 but in different 30-year windows switches between including Clusters 1 and 2, depending on which is more prevalent in each window (not shown). The resulting inconsistency is the cause of the lower stationarity visible in Figure 2. This lends additional support to the view that we are detecting significant physically consistent states; the clustering algorithm is by no means indifferent to the number of clusters we specify.

4. Conclusions

The issue of unambiguous regime identification on multidecadal time series, and of strong sensitivity of regime patterns to data and parameter changes, has caused considerable consternation and skepticism over the usefulness of the regime framework in the past. In this work we have considered the hypothesis that the near-Gaussian variability of the jet speed is a confounding factor that obscures the nonlinear regime structure of Euro-Atlantic circulation. Once the jet speed has been regressed out of the PCs of Z500, a clear, visual nonlinearity is instantly apparent in phase space. We found that K-means clustering applied in the standard way to this residual Z500 demonstrated marked improvements in statistical significance, in identifying regime number, and perhaps most importantly in interdecadal stability across the twentieth century.

It was shown that three regimes managed to capture a northern and southern jet as well as a weakly blocked state, significantly overlapping the previously identified three jet latitude regimes. Evidence supporting an extension to five regimes was also found, adding more strongly blocked states linked to a tilted and split jet in addition to the three traditional jet regimes, which also show strong stationarity. Our framework thus straight forwardly unifies both jet and circulation regimes, justifying the five-regime picture proposed in Madonna et al. (2017).

As remarked in section 3.1, removing the jet speed corresponds to removing a pattern of steady, zonal flow (NAO+). This relationship between the jet speed and zonal flow is made even clearer by stratifying the wind field into jet speed quintiles, which shows increasing jet speeds being associated with an increasingly strong zonal flow (Figure S7 in the SI). This suggests a decomposition of Euro-Atlantic circulation into a linear mode (zonal flow/NAO+) together with nonlinear, persistent deviations from this (regimes). Crucially, because the jet speed distribution does not change meaningfully when restricted to any of the five regimes (not shown), these two components are effectively independent of each other, implying that one can study the influence of both separately.

This interpretation is very similar to the one given in Woollings et al. (2008), where a bimodal framework of regimes was presented based on Rossby wave breaking. There, the NAO+ was envisaged as being a "generic," undisturbed state, while the NAO− corresponded to periods of frequent blocking events. This is entirely consistent with the clusters obtained in both Figures 3 and 4, which omit a strong NAO+ pattern in favor of a range of blocking patterns. The emergence of regime structure *after* accounting for wind speed is also explicit in Benzi et al. (1986) and Ruti et al. (2006), where evidence of bimodality only emerges for a specific range of zonal wind forcing.

With increased regime reproducibility comes increased confidence in the ability to use regime statistics as model diagnostic tools as well as providing insight into the underlying skeletal structure of nonlinearity over the Euro-Atlantic sector. In particular, this new clustering framework might be particularly suited for identifying the action of teleconnections on the North Atlantic, which can be difficult to study with either nonstationary data sets or data confined to a short, modern period. Because there is evidence that forecast models struggle to predict the jet speed (Parker et al., 2019; Strommen, 2020), there are also potential benefits of this approach to forecasting. Finally, the strong stationarity paves the way for a more robust assessment of potential future changes in regime behavior under global warming.

Data Availability Statement

The data set used (ERA20C) is publicly available online (https://www.ecmwf.int/en/forecasts/datasets/reanalysis-datasets/era-20c). The processed jet and regime indices used can be found at https://github.com/joshdorrington/ERA20C_Atlantic_variability_indices.

Acknowledgments

K. J. S. was funded by a Thomas Philips and Jocelyn Keene Junior Research Fellowship in Climate Science at Jesus College, Oxford. J. D. is funded by NERC Grant NE/L002612/1.

References

Benzi, R., Malguzzi, P., Speranza, A., & Sutera, A. (1986). The statistical properties of general atmospheric circulation: Observational evidence and a minimal theory of bimodality. *Quarterly Journal of the Royal Meteorological Society*, *112*, 661–674. https://doi.org/10.1002/qj.49711247306

Beerli, R., & Grams, C. M. (2019). Stratospheric modulation of the large-scale circulation in the Atlantic–European region and its implications for surface weather events. *Quarterly Journal of the Royal Meteorological Society*, *145*, 3732–3750. https://doi.org/10.1002/qj.3653

Cassou, C. (2008). Intraseasonal interaction between the Madden-Julian Oscillation and the North Atlantic Oscillation. *Nature*, *455*, 523–527. https://doi.org/10.1038/nature07286

Corti, S., Molteni, F., & Palmer, T. N. (1999). Signature of recent climate change in frequencies of natural atmospheric circulation regimes. *Nature*, *398*(6730), 799–802. https://doi.org/10.1038/19745

Dawson, A., Palmer, T. N., & Corti, S. (2012). Simulating regime structures in weather and climate prediction models. *Geophysical Research Letters*, *39*, L21805. https://doi.org/10.1029/2012GL053284

Falkena, S. K. J., de Wiljes, J., Weisheimer, A., & Shepherd, T. G. (2019). Revisiting the identification of wintertime atmospheric circulation regimes in the Euro-Atlantic sector. Retrieved from http://arxiv.org/abs/1912.10838

Ferranti, L., Corti, S., & Janousek, M. (2015). Flow-dependent verification of the ECMWF ensemble over the Euro-Atlantic sector. *Quarterly Journal of the Royal Meteorological Society*, *141*(688), 916–924. https://doi.org/10.1002/qj.2411

Fraley, C., Fraley, C., & Raftery, A. E. (1998). How many clusters? Which clustering method? Answers via model-based cluster analysis. *The Computer Journal*, *41*, 578–588. Retrieved from http://citeseerx.ist.psu.edu/viewdoc/summary?doi=10.1.1.7.8739

Frame, T. H., Methven, J., Gray, S. L., & Ambaum, M. H. (2013). Flow-dependent predictability of the North Atlantic jet. *Geophysical Research Letters*, *40*, 2411–2416. https://doi.org/10.1002/grl.50454

Franzke, C., Woollings, T., & Martius, O. (2011). Persistent circulation regimes and preferred regime transitions in the North Atlantic. *Journal of the Atmospheric Sciences*, *68*(12), 2809–2825. https://doi.org/10.1175/JAS-D-11-046.1

Ghil, M., & Robertson, A. W. (2002). "Waves" vs. "particles" in the atmosphere's phase space: A pathway to long-range forecasting? *Proceedings of the National Academy of Sciences of the United States of America*, *99*(SUPPL. 1), 2493–2500. https://doi.org/10.1073/pnas.012580899

Hannachi, A., Straus, D. M., Franzke, C. L., Corti, S., & Woollings, T. (2017). Low-frequency nonlinearity and regime behavior in the Northern Hemisphere extratropical atmosphere. (Vol. 55) (No. 1). https://doi.org/10.1002/2015RG000509

Madonna, E., Li, C., Grams, C. M., & Woollings, T. (2017). The link between eddy-driven jet variability and weather regimes in the North Atlantic-European sector. *Quarterly Journal of the Royal Meteorological Society*, *143*(708), 2960–2972. https://doi.org/10.1002/qj.3155

Matsueda, M., & Palmer, T. (2018). Estimates of flow-dependent predictability of wintertime Euro-Atlantic weather regimes in medium-range forecasts. *Quarterly Journal of the Royal Meteorological Society*, *144*, 1012–1027. https://doi.org/10.1002/qj.3265

Michelangeli, P. A., Vautard, R., & Legras, B. (1995). Weather regimes: Recurrence and quasi stationarity. *Journal of the Atmospheric Sciences*, *52*(8), 1237–1256. https://doi.org/10.1175/1520-0469(1995)052<1237:WRRAQS>2.0.CO;2

Palmer, T. N. (1999). A nonlinear dynamical perspective on climate prediction. *Journal of Climate*, *12*(2), 575–591. https://doi.org/10.1175/1520-0442(1999)012<0575:ANDPOC>2.0.CO;2

Parker, T., Woollings, T., Weisheimer, A., O'Reilly, C., Baker, L., & Shaffrey, L. (2019). Seasonal predictability of the winter North Atlantic Oscillation from a jet stream perspective. *Geophysical Research Letters*, *45*, 10,159–10,167. https://doi.org/10.1029/2019GL084402

Poli, P., Hersbach, H., Tan, D., Dee, D., Thépaut, J. N., Simmons, A., & Dragani, R. (2013). The data assimilation system and initial performance evaluation of the ECMWF pilot reanalysis of the 20th-century assimilating surface observations only (ERA-20C): ERA report series.

Ruti, P. M., Lucarini, V., Dell'Aquila, A., Calmanti, S., & Speranza, A. (2006). Does the subtropical jet catalyze the midlatitude atmospheric regimes? *Geophysical Research Letters*, *33*, L06814. https://doi.org/10.1029/2005GL024620

Schwarz, G. (1978). Estimating the dimension of a model, *6*(2), 461–464. https://doi.org/10.1214/AOS/1176344136

Straus, D. M. (2010). Synoptic-eddy feedbacks and circulation regime analysis. *Monthly Weather Review*, *138*(11), 4026–4034. https://doi.org/10.1175/2010MWR3333.1

Straus, D. M., Corti, S., & Molteni, F. (2007). Circulation regimes: Chaotic variability versus SST-forced predictability. *Journal of Climate*, *20*(10), 2251–2272. https://doi.org/10.1175/JCLI4070.1

Strommen, K. (2020). Jet latitude regimes and the predictability of the North Atlantic Oscillation. *Quarterly Journal of the Royal Meteorological Society*, 1–24. https://doi.org/10.1002/qj.3796

Strommen, K., Mavilia, I., Corti, S., Matsueda, M., Davini, P., von Hardenberg, J., & Mizuta, R. (2019). The sensitivity of Euro-Atlantic regimes to model horizontal resolution. *Geophysical Research Letters*, *46*, 7810–7818. https://doi.org/10.1029/2019GL082843

Strommen, K., & Palmer, T. N. (2019). Signal and noise in regime systems: A hypothesis on the predictability of the North Atlantic Oscillation. *Quarterly Journal of the Royal Meteorological Society*, *145*, 147–163. https://doi.org/10.1002/qj.3414

Vautard, R. (1990). Multiple weather regimes over the North Atlantic: Analysis of precursors and successors. *Monthly Weather Review*, *118*, 2056–2081. https://doi.org/10.1175/1520-0493(1990)118<2056:MWROTN>2.0.CO;2

Woollings, T., Charlton-Perez, A., Ineson, S., Marshall, A. G., & Masato, G. (2010). Associations between stratospheric variability and tropospheric blocking. *Journal of Geophysical Research*, *115*, D06108. https://doi.org/10.1029/2009JD012742

Woollings, T., Czuchnicki, C., & Franzke, C. (2014). Twentieth century North Atlantic jet variability. *Quarterly Journal of the Royal Meteorological Society*, *140*(680), 783–791. https://doi.org/10.1002/qj.2197

Woollings, T., Hannachi, A., & Hoskins, B. (2010). Variability of the North Atlantic eddy-driven jet stream. *Quarterly Journal of the Royal Meteorological Society*, *136*(649), 856–868. https://doi.org/10.1002/qj.625

Woollings, T., Hannachi, A., Hoskins, B., & Turner, A. (2010). A regime view of the North Atlantic oscillation and its response to anthropogenic forcing. *Journal of Climate*, *23*(6), 1291–1307. https://doi.org/10.1175/2009JCLI3087.1

Woollings, T., Hoskins, B., Blackburn, M., & Berrisford, P. (2008). A new Rossby wave breaking interpretation of the North Atlantic Oscillation. *Journal of the Atmospheric Sciences*, *65*(2), 609–626. https://doi.org/10.1175/2007JAS2347.1